Recovery of Boundary Image Sticking Using Aging Discharge in AC Plasma Display Panel

Choon-Sang Park, Heung-Sik Tae, *Senior Member, IEEE*, Young-Kuk Kwon, and Eun Gi Heo

***Abstract*—A full-white aging discharge process is proposed to recover permanent boundary image sticking in an ac plasma display panel. A simultaneous 100-h aging discharge in both boundary image sticking and nonimage sticking cells induced sputtering and redeposition of the MgO surfaces in both cell types, resulting in similar MgO surface morphologies. The luminance characteristics, including the infrared emission and chromaticity coordinates, of the boundary image sticking cells were also compared to those of the nonimage sticking cells. As a result, the full-white aging discharge was found to contribute to the recovery of permanent boundary image sticking cells.**

***Index Terms*—Full-white aging discharge, permanent boundary image sticking, redeposition of Mg, scanning electron microscope (SEM) analyses, time-of-flight secondary ion mass spectrometry (TOF-SIMS), V_t close curve, 42-in ac-plasma display panel (PDP) module.**

I. Introduction

THE REALIZATION of high-quality plasma display panels (PDPs) requires an urgent solution to the image sticking or image retention problems induced in PDP cells after strong sustain discharges have been repeatedly produced during a sustain period [1]–[9]. Image retention means temporal image sticking that is easily recoverable through minor treatment, whereas image sticking is permanent and not recoverable even with severe treatment. Image sticking is also known to be induced in the nondischarge cells adjacent to the discharge cells, in which case it is called halo-type boundary image sticking [10], [11]. Previous experimental results have shown that the main culprit inducing permanent image sticking is the Mg sputtered from the MgO surfaces of the discharge cells due to the severe ion bombardment during a sustain discharge [10]–[12]. The deposition of the sputtered Mg on the phosphor layer of the discharge cells, or the redeposition of the sputtered Mg on the MgO surface of the nondischarge cells adjacent to the discharge cells, can alter the reset or sustain-discharge characteristics, thereby causing image sticking or boundary image sticking [10]–[12].

Accordingly, this paper investigated the effects of a full-white aging discharge on the recovery of boundary image sticking. The luminance, infrared (IR) (828 nm) emission, and voltage threshold (V_t) close curve of a nondischarge region adjacent to the discharge region were all observed in comparison with those of a nondischarge region far away from the discharge region using two different image patterns (dark and full-white backgrounds) after a 100-h full-white aging discharge in a 42-in ac-PDP module. In addition, scanning electron microscope (SEM) and time-of-flight secondary ion mass spectrometry (TOF-SIMS) were used to inspect the surface morphology of the MgO layer and to analyze the Mg species deposited on the phosphor layer, respectively, after the 100-h full-white aging discharge.

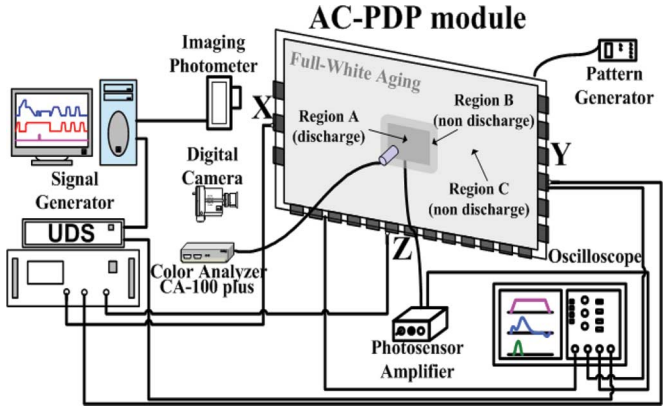

Fig. 1. Schematic diagram of experimental setup employed in this paper.

II. Experimental Setup

Fig. 1 shows the optical measurement systems and commercial 42-in ac-PDP module with three electrodes used in the experiment, where X is the sustain electrode, Y is the scan electrode, and Z is the address electrode. A color analyzer (CA-100 Plus), an imaging photometer (Prometric PM Series), a pattern generator, a signal generator, and a photosensor amplifier (Hamamatsu C6386) were used to measure the luminance, IR emission, and V_t close curve, respectively. To produce the boundary image sticking, the entire region of the 42-in panel was changed to a dark background (about 0.1 cd/m^2) or a full-white background (about 175 cd/m^2) immediately after displaying a square-type image (region A) at a peak luminance (about 1000 cd/m^2) for about 500 h. Using the automatic power control system of the PDP, 1520 sustain pulses were alternately applied to the X and Y electrodes during one TV field $(= 16.67$ ms) to display a square-type test image with a 1% display region within the entire region of the 42-in panel. As a result, the 500-h strong sustain discharge in region A induced both permanent

Manuscript received March 13, 2007; revised June 20, 2007. This work was supported in part by the New Growth Engine project of the Ministry of Commerce, Industry, and Energy of Korea and the Brain Korea 21.

C.-S. Park and H.-S. Tae are with the School of Electrical Engineering and Computer Science, Kyungpook National University, Daegu 702-701, Korea (e-mail: hstae@ee.knu.ac.kr).

Y.-K. Kwon and E. G. Heo are with the Plasma Display Panel Division, Samsung SDI Company, Ltd., Cheonan City 330-300, Korea.

Color versions of one or more of the figures in this paper are available online at http://ieeexplore.ieee.org.

Digital Object Identifier 10.1109/TPS.2007.905208

TABLE I
COMPARISON OF IMAGE-STICKING PRODUCTION CONDITIONS AND FULL-WHITE AGING DISCHARGE CONDITIONS

	Displayed area	Pulse number per 1-TV field (16.67ms)	Total discharge time
Image sticking production condition	5cm×6cm in 42-inch	1520	500 hours
Full-white aging condition	Entire in 42-inch	300	100 hours

TABLE II
SPECIFICATIONS OF 42-in AC PDP USED IN THIS PAPER

Front Panel		Rear Panel	
ITO width	225 μm	Barrier rib width	55 μm
ITO gap	85 μm	Barrier rib height	120 μm
Bus width	50 μm	Address width	95 μm
Pixel Pitch		912 × 693 μm	
Gas chemistry		Ne-Xe (15 %)-He (35 %)	
Barrier rib type		Closed rib	

image sticking in region A and permanent boundary image sticking in region B. To eliminate the boundary image sticking in region B resulting from the 500-h strong sustain discharge in region A, a full-white aging discharge (about 175 cd/m^2) was continually produced for about 100-h across the entire region of the 42-in ac-PDP module. Meanwhile, 300 sustain pulses were alternately applied to the X and Y electrodes per one TV field during the full-white aging discharge.

Table I compares the image sticking production condition and the full-white aging discharge condition. To check on the removal of the boundary image sticking, the entire region of the 42-in panel was changed to dark background and full-white background images immediately after the 100-h full-white aging discharge. The frequency for the sustain period was 200 kHz, and the sustain voltage was 205 V. A driving method with a selective reset waveform was also adopted, and the gas chemistry in the experiment was Ne–Xe (15%)–He (35%). The detailed panel specifications are listed in Table II.

III. EXPERIMENTAL OBSERVATION OF BOUNDARY IMAGE STICKING RECOVERY USING AGING DISCHARGE

A. *Monitoring of Luminance*

Figs. 2 and 3 show the luminance difference among three regions—A, B, and C—observed under dark background and full-white background images before and after the full-white aging discharge. Before the full-white aging discharge, image sticking occurred in regions A and B under a dark background, as shown in Fig. 2(c). The luminance of region A (the discharge region with the image sticking cells) was observed to be higher than that of the nondischarge region C (the nondischarge region). However, region B (the nondischarge region adjacent to the discharge region) showed the highest luminance under a dark background. As shown in Fig. 3(c), image sticking also occurred in regions A and B under a full-white background, although the luminance of region B was observed to be lower than that of region C or A, in contrast to the case of a dark background.

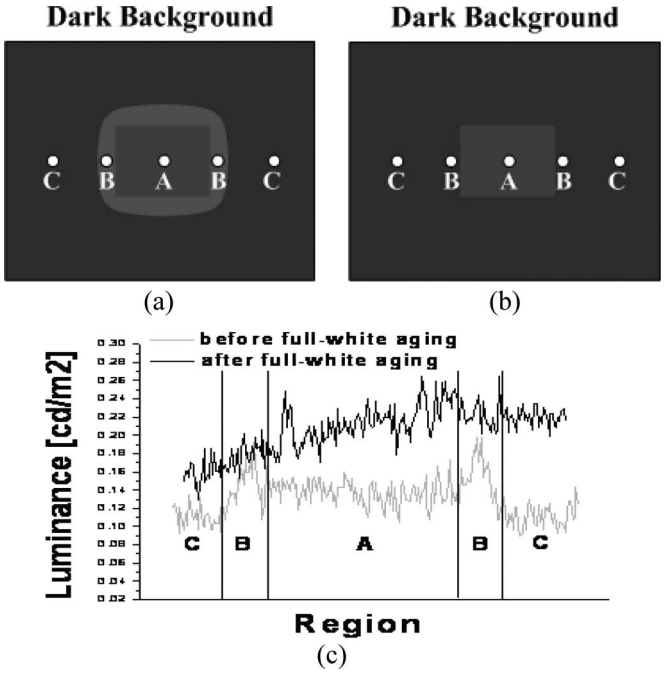

Fig. 2. Image sticking pattern under dark background captured from test panel (a) before full-white aging and (b) after full-white aging discharge, plus (c) luminance difference among regions A, B, and C before and after full-white aging discharge.

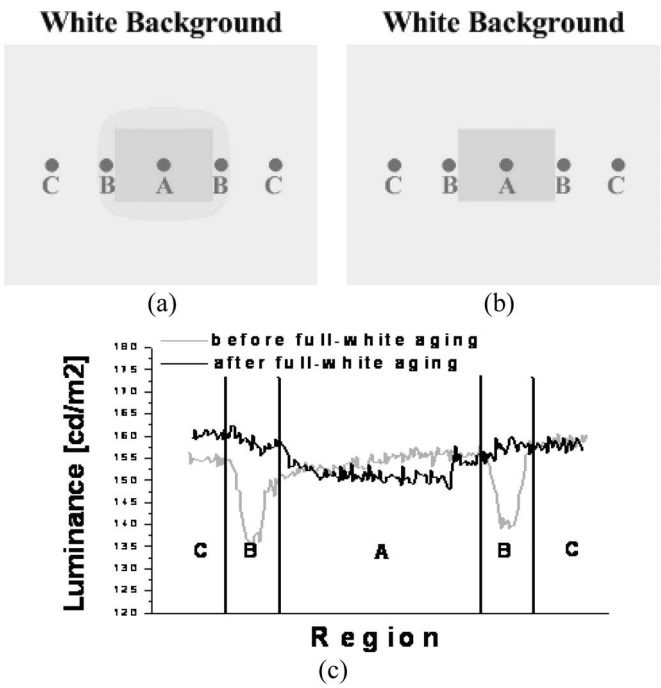

Fig. 3. Image sticking pattern under full-white background captured from test panel (a) before full-white aging and (b) after full-white aging discharge, plus (c) luminance difference among regions A, B, and C before and after full-white aging discharge.

In region A, where the strong sustain discharge was repeatedly produced, Mg species were sputtered from the MgO surface due to the bombardment of ions onto the MgO protective layer during the iterant strong sustain discharge, meaning that the Mg species were predominantly redeposited on the phosphor layers of the cells in region A. Furthermore, the MgO

surfaces in region A were changed into damaged MgO surfaces due to the severe ion bombardment, causing a slight increase in the firing voltage under MgO-cathode conditions. Meanwhile, the redeposition of the Mg on the phosphor layer contributed to the enhancement of the plate gap discharge, particularly under phosphor-cathode conditions, thereby increasing the IR emission during the reset period and even during the sustain period. However, the redeposition of the Mg on the phosphor layer prohibited the visible conversion of the phosphor layer, thereby decreasing the luminance. In region B, with no sustain discharge, yet located near region A, the Mg was transported from the adjacent cells where the MgO surface was sputtered and redeposited on both the MgO surface and the phosphor layer. The redeposited Mg on the MgO surface and phosphor layer in region B then contributed to the enhancement of both the surface and the plate gap discharges, thereby increasing the IR emission during the reset and sustain periods. However, as in region A, the redeposition of the Mg on the phosphor layer in region B prohibited the visible conversion of the phosphor layer, thereby decreasing the luminance [10], [11]. Nonetheless, after the 100-h full-white aging discharge, the image pattern and the luminance of regions B and C were observed to be almost the same under the dark and full-white backgrounds, as shown in Figs. 2(c) and 3(c), confirming that the full-white aging discharge recovered the luminance characteristics of the boundary image sticking cells.

B. Monitoring of IR Emission

Fig. 4 shows the changes in the IR (828 nm) emissions measured from regions A, B, and C during the reset period under a dark background when using just a weak reset discharge. Before the full-white aging discharge, the IR peak in region B was observed to be shifted to the left when compared with that in region C, as shown in Fig. 4(a), indicating an efficient initiation of the weak reset discharge at a lower starting discharge voltage during the reset period. However, after the full-white aging discharge, the ignition time and intensity of the IR (828 nm) emission waveforms showed no difference between regions B and C, as shown in Fig. 4(b).

Fig. 5 shows the changes in the IR (828 nm) emissions measured from regions A, B, and C during the sustain period to investigate the IR emission characteristics under a full-white background. Slightly asymmetric IR emission intensities were measured depending on whether the sustain waveform was applied to the X or Y electrode; however, this was not related to the image sticking phenomenon. The IR emission data in Fig. 5 reveal that the IR peaks for regions A and B were intensified compared with those for region C. Yet, after the full-white aging discharge, the ignition time and intensity of the IR (828 nm) emission waveforms showed no difference between regions B and C, as shown in Fig. 5(b), confirming that the full-white aging discharge recovered the IR emission characteristics of the boundary image sticking cells.

C. Monitoring of Firing Voltage Using V_t Close Curves

To identify the main factor responsible for recovering the differences in the luminance and IR characteristics between

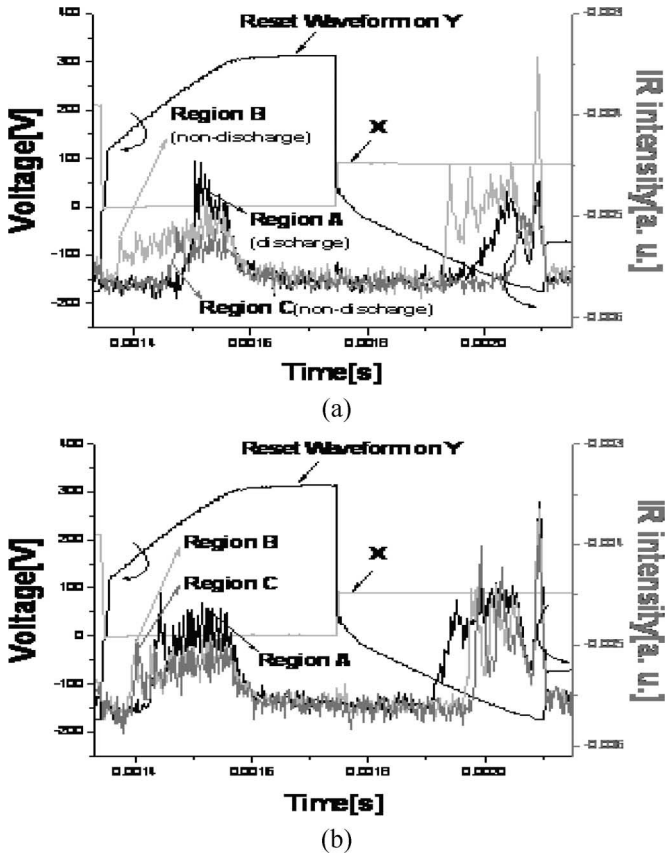

Fig. 4. Comparison of IR (828 nm) emissions from regions A, B, and C during reset period under dark background. (a) Before full-white aging discharge. (b) After full-white aging discharge.

regions B and C after the 100-h full-white aging discharge, the V_t close curves were measured in regions A, B, and C.

Table III shows the detailed changes in the firing voltages obtained from the V_t close curves measured for regions A, B, and C. Before the full-white aging discharge, the firing voltages under a phosphor-cathode condition and under an MgO-cathode condition in region B were slightly decreased by about 10–12 and 8–16 V, respectively, in comparison with those in region C, as shown in Fig. 6(a) and Table III. The reduction of the firing voltage in the surface and plate gap discharges was presumably due to the Mg deposition on the MgO and phosphor layers, which was caused by the MgO sputtering induced by the iterant strong sustain discharge in region A [10], [11]. However, after the full-white aging discharge, the differences in the firing voltage under the phosphor- and MgO-cathode conditions in regions B and C decreased by about 2–6 and 2–8 V, respectively, in comparison with those before the full-white aging discharge, even though the firing voltage conditions in region A remained almost constant before the full-white aging discharge, as shown in Fig. 6(b) and Table III. Consequently, this confirms that the full-white aging discharge contributed to the recovery of the firing voltage conditions of the boundary image sticking cells.

D. Monitoring of Deposition of Sputtered Mg on Phosphor Layer and Change in Surface Morphology of MgO Layer

SEM and TOF-SIMS were used to inspect the changes in the surface morphology of the MgO layer and to analyze the Mg

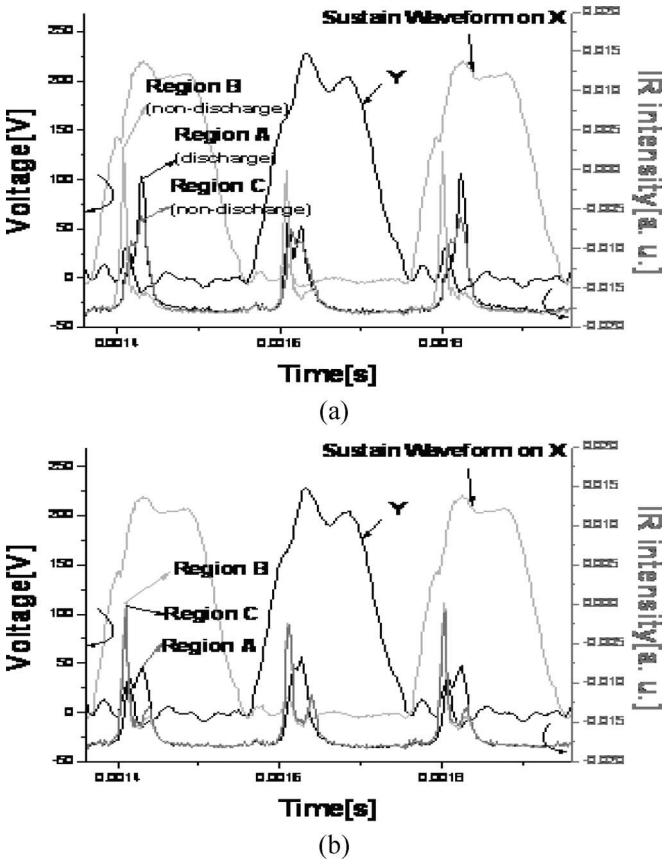

Fig. 5. Comparison of IR (828 nm) emissions from regions A, B, and C during sustain period under full-white background. (a) Before full-white aging discharge. (b) After full-white aging discharge.

TABLE III
CHANGES IN FIRING VOLTAGES MEASURED UNDER MgO-CATHODE AND PHOSPHOR-CATHODE CONDITIONS USING V_t CLOSE CURVE METHOD BEFORE AND AFTER FULL-WHITE AGING DISCHARGE

Sides			Firing voltage		
			region A	region B	region C
Before full-white aging	MgO Cathode	I (X-Y)	262	256	272
		II (Z-Y)	188	174	182
		III (Z-X)	210	196	204
		IV (Y-X)	312	294	306
	Phosphor Cathode	V (Y-Z)	236	336	346
		VI (X-Z)	232	332	344
After full-white aging	MgO Cathode	I (X-Y)	278	262	270
		II (Z-Y)	192	182	186
		III (Z-X)	214	202	204
		IV (Y-X)	322	312	316
	Phosphor Cathode	V (Y-Z)	238	344	346
		VI (X-Z)	228	334	340

deposited on the phosphor layer, respectively, before and after the 100-h full-white aging discharge.

Fig. 7(a) and (b) shows the SEM images captured from regions A, B, and C before and after the full-white aging discharge. Before the full-white aging discharge, in region A, the MgO surface was sputtered or damaged due to the severe ion bombardment during the 500-h strong sustain discharge, resulting in a relatively large grain size. In region C, which was the nondischarge region far away from the discharge region, the MgO surface remained unchanged, maintaining a small grain

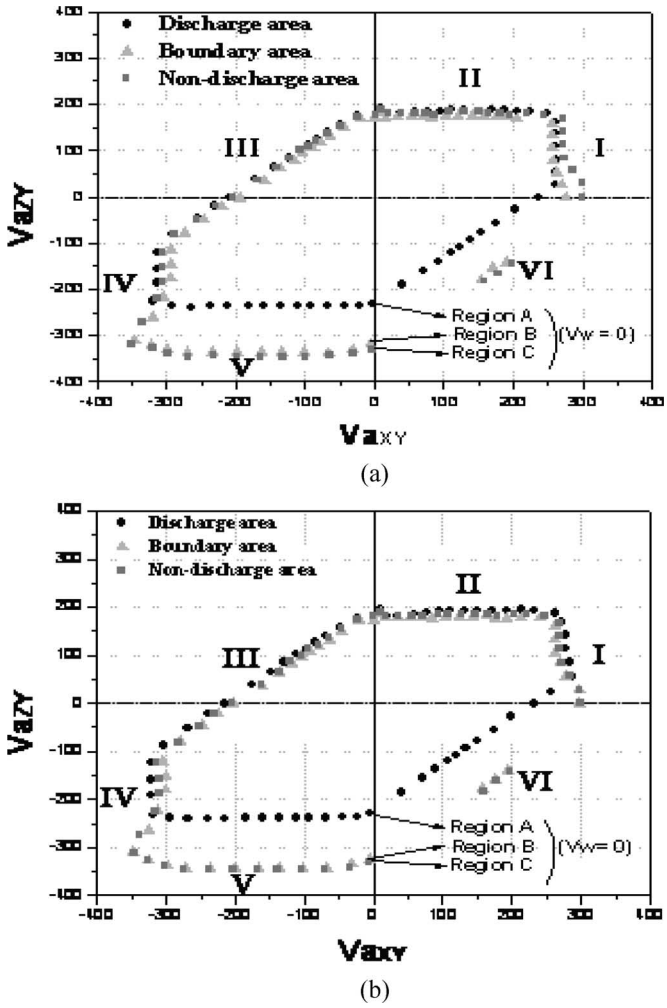

Fig. 6. Comparison of V_t close curves for regions A, B, and C without initial wall charges. (a) Before full-white aging discharge. (b) After full-white aging discharge.

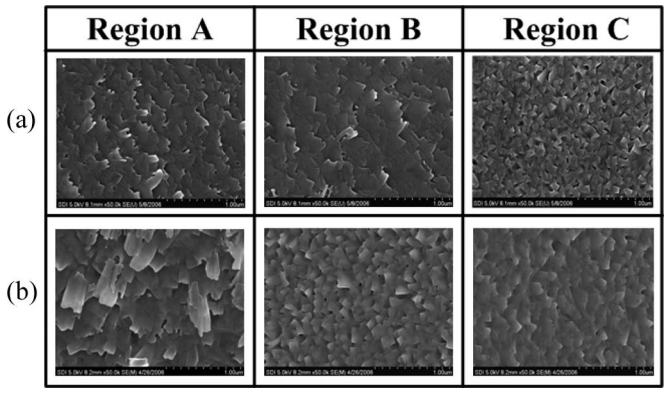

Fig. 7. Comparison of MgO-surface SEM images of regions A, B, and C. (a) Before full-white aging discharge. (b) After full-white aging discharge.

size. In region B, which was the nondischarge region adjacent to the discharge region, since there was no discharge in this region, it was expected that the morphology of the MgO surface would remain unchanged, such as that in region C. However, as shown in Fig. 7(a), the morphology of the MgO surface in region B was similar to that in region A with a relatively large grain size. This phenomenon in region B seemed to occur

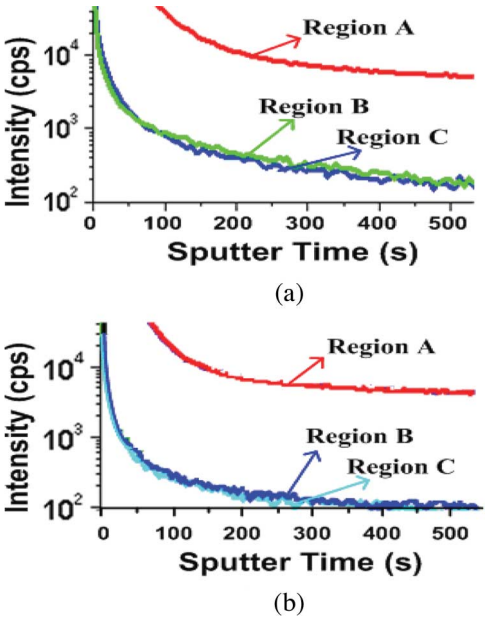

Fig. 8. Comparison of Mg profiles for red phosphor layer in regions A, B, and C based on TOF-SIMS analysis. (a) Before full-white aging discharge. (b) After full-white aging discharge.

due to the redeposition of the Mg transported from region A, where the MgO surface was sputtered during the iterant strong sustain discharge. During the full-white aging discharge, the ions bombarded the MgO surfaces in all three regions: A, B, and C. As shown in Fig. 7(b), the resultant MgO surface in region A, i.e., the image sticking region, became rougher with a larger grain size. However, in region B (the boundary image-sticking region), the MgO surface revealed a smaller grain size after the full-white discharge with a similar surface morphology to the MgO layer in region C. In regions B and C, the sustain discharges were simultaneously produced for 100 h under the full-white aging discharge condition, yet the ion bombardment was less intense than that under the 500-h sustain discharge for displaying the test image with a 1% display area. Thus, the surface morphologies of the MgO layers in regions B and C became similar as a result of the full-white aging discharge, as shown in Fig. 7(b). Therefore, the SEM images in Fig. 7(b) confirmed that the simultaneous ion bombardment under the full-white aging discharge caused the MgO surfaces in regions B and C, particularly the redeposited MgO surface in region B, to equalize.

Fig. 8 shows a comparison of the Mg profiles on the red phosphor layer for regions A, B, and C when using the TOF-SIMS analysis. In Fig. 8, the Mg profile means the intensity of the Mg sputtered from the red phosphor layer according to the operating time during which Ar ions struck the surface of the red phosphor layer. Before the full-white aging discharge, the Mg intensity in regions A and B shifted upward compared with that in region C, as shown in Fig. 8(a), indicating that the Mg was redeposited on the phosphor layer. Although the sputtered Mg was predominantly redeposited in region A (the discharge region), there was also a slight redeposition in region B (the nondischarge region adjacent to the discharge region). The redeposition of the Mg on the phosphor layer significantly affected the discharge characteristics, particularly under phosphor-cathode conditions. Therefore, the firing voltage in region A, where the sputtered Mg was predominantly redeposited, was the lowest, as shown in the V_t close curve analysis in Fig. 6. Furthermore, the firing voltage in region B, where the sputtered Mg was slightly redeposited, was lower than that in region C (the nondischarge region), where the sputtered Mg was not redeposited. However, after the full-white aging discharge, the Mg intensity in region B was almost similar to that for the cells in region C, indicating that the 100-h full-white aging discharge contributed to recovering the boundary image sticking.

TABLE IV
CIE (1931) CHROMATICITY COORDINATES AND COLOR TEMPERATURES FOR REGIONS A, B, AND C BEFORE AND AFTER FULL-WHITE AGING DISCHARGE

			region A	region B	region C
Before full-white aging	Chromaticity coordinates	x	0.2806	0.2777	0.2811
		y	0.2922	0.2721	0.2818
	Color temperature, T[K]		9818	11667	10444
After full-white aging	Chromaticity coordinates	x	0.2910	0.2817	0.2810
		y	0.2957	0.2814	0.2823
	Color temperature, T[K]		8636	10333	10333

E. Monitoring of Chromaticity Coordinates and Color Temperature

Table IV shows the Commission Internationale de l'Eclairage (International Commission on Illumination—CIE) chromaticity coordinates and related color temperatures measured for regions A, B, and C. Before the full-white aging discharge, as shown in Table IV, the x and y chromaticity coordinates and color temperatures changed for both the image-sticking cells in region A and the boundary image-sticking cells in region B. However, after the full-white aging discharge, the x and y chromaticity coordinates and color temperatures in region B were almost the same as those in region C, thereby confirming that the full-white aging discharge contributed to the recovery of the color characteristics of the light emitted from the red, green, and blue cells in the boundary image-sticking region (region B).

F. Schematic Model Describing Recovery of Permanent Boundary Image Sticking Phenomenon

Based on the experimental results obtained from the V_t close curve, SEM, and TOF-SIMS analyses before and after the full-white aging discharge, Fig. 9 shows a schematic model that describes the recovery of the permanent boundary image sticking phenomenon. As shown in Fig. 9(a), the image sticking problem, including the boundary image sticking problem, is mainly caused by the sputtering of the MgO protective layer due to the iterant strong ion bombardment, resulting in redeposition on the MgO surface or deposition on the phosphor layer [10], [11]. Before the full-white aging discharge, region A (the discharge region) was the predominant location for sputtering of the MgO surface, causing severe damage to the MgO surface,

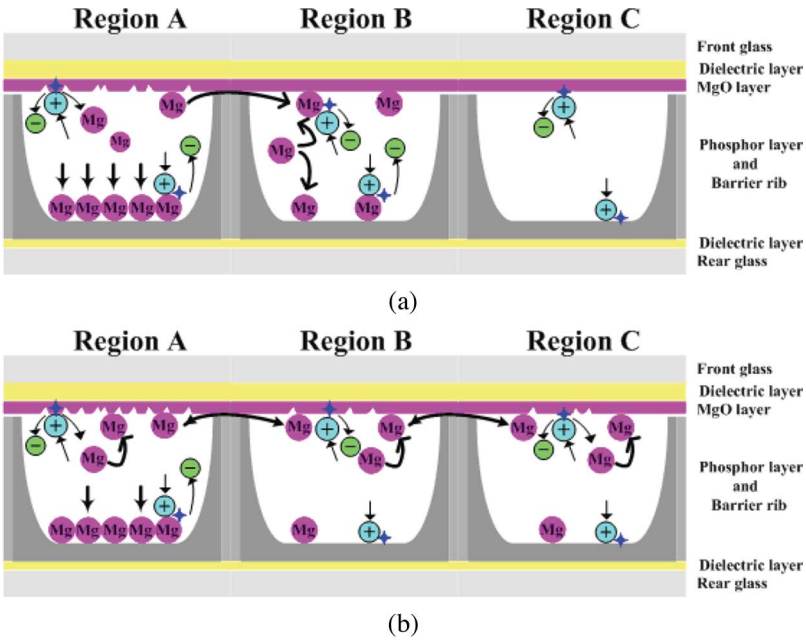

Fig. 9. Schematic model of recovery of permanent boundary image sticking phenomenon for regions A, B, and C. (a) Before full-white aging discharge. (b) After full-white aging discharge.

plus a large amount of Mg was detected from the phosphor layer. Meanwhile, in region B (the nondischarge region adjacent to the discharge region), the morphology of the MgO surface was similar to that in region A, which was caused by redeposition of the MgO surface due to transportation of the Mg sputtered from region A (the discharge region). Nonetheless, even though the morphologies of the MgO surfaces in regions A and B were found to be similar before the full-white aging discharge, the states of the MgO surfaces were quite different, as the MgO surface in region A was a damaged or sputtered layer, whereas the MgO surface in region B was a redeposited layer. During the full-white aging discharge, the ions stroked all the MgO surfaces in regions A, B, and C. However, although the sputtering and redeposition of the MgO surface occurred simultaneously in all the three regions, as shown in Fig. 9(b), since the initial states of the MgO surfaces in regions A, B, and C were quite different, as shown in Fig. 9(a), the resultant MgO surfaces showed different surface morphologies after the full-white aging discharge. As a result of the 100-h full-white aging discharge, the MgO surface in region A was more sputtered, and its grain size was larger. In contrast, the redeposited MgO surface in region B was only slightly sputtered, and its grain size was smaller when compared with that before the full-white aging discharge. In region C, the MgO surface was also slightly sputtered, and its grain size was slightly large. Finally, the morphologies of the MgO surfaces in regions B and C were found to be similar after the full-white aging discharge, indicating a recovery of the boundary image sticking cells (region B) into normally working cells (region C).

IV. Conclusion

When displaying a square-type test image with a peak luminance for 500-h on a 42-in plasma TV, permanent image sticking and boundary image sticking were produced. A full-white aging discharge was then proposed to recover the permanent boundary image sticking. SEM images showed that the surface morphologies of the MgO layers in regions B (boundary image-sticking cells) and C (normally working cells) became similar after a 100-h full-white aging discharge. Meanwhile, from a TOF-SIMS analysis, the Mg intensities detected from the red phosphor layers in regions B and C were almost the same. In addition, the resultant luminance and IR emission characteristics also exhibited no difference between region B (boundary image-sticking cells) and region C (normally working cells). Furthermore, a V_t close curve analysis showed that the firing voltage differences under MgO-cathode and phosphor-cathode conditions between regions B and C were significantly reduced to within 2–8 V. Finally, the x and y chromaticity coordinates and color temperature in region B were almost the same as those in region C. Consequently, the results confirm that a full-white aging discharge can contribute to the recovery of permanent boundary image-sticking cells into normally working cells.

References

[1] J.-W. Han, H.-S. Tae, B. J. Shin, S.-I. Chien, and D. H. Lee, "Experimental observation of temperature-dependent characteristics for temporal dark boundary image sticking in 42-in. AC-plasma display panel," *IEEE Trans. Plasma Sci.*, vol. 34, no. 2, pp. 324–330, Apr. 2006.

[2] H.-S. Tae, C.-S. Park, B.-G. Cho, J.-W. Han, B. J. Shin, S.-I. Chien, and D. H. Lee, "Driving waveform for reducing temporal dark image sticking in AC plasma display panel based on perceived luminance," *IEEE Trans. Plasma Sci.*, vol. 34, no. 3, pp. 996–1003, Jun. 2006.

[3] L. C. Pitchford, J. Wang, D. Piscitelli, and J.-P. Boeuf, "Ion and neutral energy distribution to the MgO surface and sputtering rates in plasma display panel cells," *IEEE Trans. Plasma Sci.*, vol. 34, no. 2, pp. 351–359, Apr. 2006.

[4] T. Kosaka, K. Sakita, and K. Betsui, "Firing voltage fluctuation phenomenon caused by gas density nonuniformity in PDPs," in *Proc. IDW/AD Dig.*, 2005, pp. 1469–1472.

[5] H.-S. Tae, J.-W. Han, S.-H. Jang, B.-N. Kim, B. J. Shin, B.-G. Cho, and S.-I. Chien, "Experimental observation of image sticking phenomenon

in AC plasma display panel," *IEEE Trans. Plasma Sci.*, vol. 32, no. 6, pp. 2189–2196, Dec. 2004.
[6] J. H. Choi, Y. Jung, K. B. Jung, S. B. Kim, P. Y. Oh, H. S. Jung, K. Y. Sung, and E. H. Choi, "Influence of image sticking on electro-optical characteristics in alternating-current plasma display panels," in *Proc. IDW Dig.*, 2003, pp. 913–916.
[7] H.-S. Tae, J.-W. Han, B.-G. Cho, and S.-I. Chien, "Temporal image sticking phenomena and reducing methods in AC PDP," in *Proc. IMID Dig.*, 2004, pp. 176–179.
[8] H.-J. Lee, D.-H. Kim, Y.-R. Kim, M.-S. Hahm, D.-K. Lee, J.-Y. Choi, C.-H. Park, J.-W. Rhyu, J.-K. Kim, and S.-G. Lee, "Analysis of temporal image sticking in AC-PDP and the methods to reduce it," in *Proc. SID Dig.*, 2004, pp. 214–217.
[9] B. J. Shin, K. C. Choi, and J. H. Seo, "Effects of pre-reset conditions on reset discharge from ramp reset waveforms in AC plasma display panel," *IEEE Trans. Electron Devices*, vol. 52, no. 1, pp. 17–22, Jan. 2005.
[10] C.-S. Park, H.-S. Tae, Y.-K. Kwon, S. B. Seo, E. G. Heo, B.-H. Lee, and K. S. Lee, "Experimental study on halo-type boundary image sticking in 42-in. AC-plasma display panel," in *Proc. SID Dig.*, 2006, pp. 1213–1216.
[11] C.-S. Park, H.-S. Tae, Y.-K. Kwon, and E. G. Heo, "Experimental observation of halo-type boundary image sticking in AC plasma display panel," *IEEE Trans. Electron Devices*, vol. 54, no. 6, pp. 1315–1320, Jun. 2007.
[12] Y.-G. Han, S. B. Lee, C. G. Son, S. H. Jeong, N. L. Yoo, H. J. Lee, J. H. Lee, K. B. Song, B. D. Ko, J. M. Jeong, P. Y. Oh, M. W. Moon, K. B. Jung, and E. H. Choi, "An optical characteristics for image sticking in AC-plasma display panel," in *Proc. IDW/ASID Dig.*, 2005, pp. 485–488.

Choon-Sang Park received the M.S. degree in electronic and electrical engineering from Kyungpook National University, Daegu, Korea, in 2006, where he is currently working toward the Ph.D. degree in electronic engineering.

He is currently with the School of Electrical Engineering and Computer Science, Kyungpook National University. His current research interests include plasma physics and driving waveform of plasma display panels.

Heung-Sik Tae (M'00–SM'05) received the B.S., M.S., and Ph.D. degrees in electrical engineering from Seoul National University, Seoul, Korea, in 1986, 1988, and 1994, respectively.

Since 1995, he has been a Professor with the School of Electrical Engineering and Computer Science, Kyungpook National University, Daegu, Korea. His research interests include optical characterization and driving waveform of plasma display panels, design of millimeter-wave guiding structures, and electromagnetic wave propagation using metamaterial.

Dr. Tae is a member of the Society for Information Display. He has been serving as an Editor for the IEEE TRANSACTIONS ON ELECTRON DEVICES section on display technology since 2005.

Young-Kuk Kwon received the B.S. degree in chemical science from Keimyung University, Daegu, Korea, in 1995 and the M.S. degree in chemical science from Kyungpook National University, Daegu, in 1997.

He is currently a Manager with the Plasma Display Panel (PDP) Division, Samsung SDI Company, Ltd., Cheonan City, Korea. His current research interests include plasma discharge and panel design of PDPs.

Eun-Gi Heo received the B.S. degree in physical science from Seoul National University, Seoul, Korea, in 1988 and the M.S. and Ph.D. degrees from Korea Advanced Institute of Science and Technology, Taejon, Korea, in 1990 and 1996, respectively.

He is currently a General Manager with the Development Team, Plasma Display Panel Division, Samsung SDI Company, Ltd., Cheonan City, Korea. His current research interests include plasma physics and panel design of PDPs.